Electronic Supplementary Information

Cavity structured S-NiO with Improved Energy Density for Aqueous Asymmetric Hybrid Supercapacitor by CDA mechanism

Pratik Ashok Patil†[a], Suraj Anandrao Khalate[b], Umakant Mahadev Patil[b], Rajendra Devidas Kale[a], Sachin Babasaheb Kulkarni†*[a]

[a.] *Advanced Electrochemical Laboratory, Department of Physics, Tuljaram Chaturchand College, Baramati (MH) India-413102.*
[b.] *Centre for Interdisciplinary Research, D. Y. Patil Education Society, Kolhapur-416 006, India.*
† Equally contributed authors,
*Corresponding Author E-mail Address: sachinkulkarni21@gmail.com

1. Structural studies:

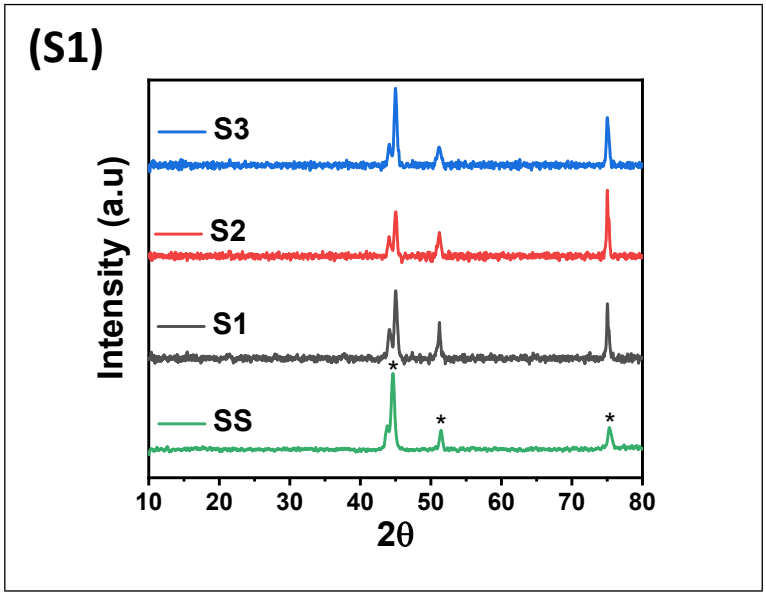

Fig S1. Shows X-ray diffraction patterns of as synthesised thin films deposited at different quantity of complexing agent 10, 20 & 30 ml namely as S1, S2 and S3, also SS refers to stainless steel substrate.

Structural study provides information about crystalline size (D), inter-atomic spacing, Micro strain (Ɛ) and Dislocation density (δ) have been calculated.

The average crystalline size is calculated by Debye–Scherrer's equation

$$\mathbf{D} = \frac{K\lambda}{\beta \cos\theta} \qquad \mathbf{(1)}$$

Where, D is size of crystallites, K is crystallite shape factor a fine estimate is 0.9, λ is wavelength of X-ray, β is (FWHM) full width at half the maximum in radians of the X-ray diffraction peak & θ which is Braggs' angle (deg.). Investigation of Inter-planer d_{hkl} Spacing which also known as the lattice parameters a, b, and c for cubic phase was determine using following equation 5.

$$\frac{1}{d_{hkl}^2} = \frac{h^2 + k^2 + l^2}{a^2} \qquad \textbf{(2)}$$

Lattice constants were found to be a = 4.1771 Å values according to standard JCPDS card no. 47-1049. The origin of the micro-strain is related to the lattice misfit, which in turn depends upon the deposition conditions. The micro-strain (ε) and dislocation density (δ) calculated using following Equation 6 & 7.

$$\boldsymbol{\varepsilon} = {}^{\beta\, COS\, \theta}/_{4} \qquad \textbf{(3)}$$

$$\boldsymbol{\delta} = \frac{1}{D^2} \qquad \textbf{(4)}$$

Where δ (length of dislocation per unit volume (lines m^{-2}), Microstructure observations such as crystallite size and micro-strain were obtained using an X-ray diffraction pattern (XRD) of S-NiO thin films. Micro-strain is mainly depending on defects like crystallite boundaries and twin boundaries. In the form of limited micro-strain, Nano-crystalline contain huge amount of stored energy.

Sample	Position [2θ °]	h	k	l	d-spacing [Å] (Standard)	d-spacing [Å] (Calculated)	Crystalline size (D) nm	Dislocation Density (δ)	Micro-Strain (ε)	Band Gap (eV)
A1	37.2697	1	1	1	2.41268	2.4152	**32.87**	**0.0009**	**0.0008**	**2.05**
	43.7512	2	0	0	2.06912	2.0713				
	62.818	2	2	0	1.47932	1.4835				
	79.31	2	2	2	1.20615	1.20751				
A2	37.3057	1	1	1	2.40794	2.40746	28.38	0.0012	0.0009	2.36
	43.8033	2	0	0	2.06454	2.08837				
	62.8812	2	2	0	1.47798	1.49973				
	79.3694	2	2	2	1.20617	1.2135				
A3	37.3367	1	1	1	2.4085	2.4116	26.84	0.0013	0.001	2.45
	43.8433	2	0	0	2.06498	2.0957				
	62.8874	2	2	0	1.47785	1.4866				
	79.4094	2	2	2	1.20717	1.2145				

Table.ST1 The microstructural values of annealed A1, A2 & A3 electrodes.

2. Morphological investigation of as synthesised electrodes (S1, S2 & S3):

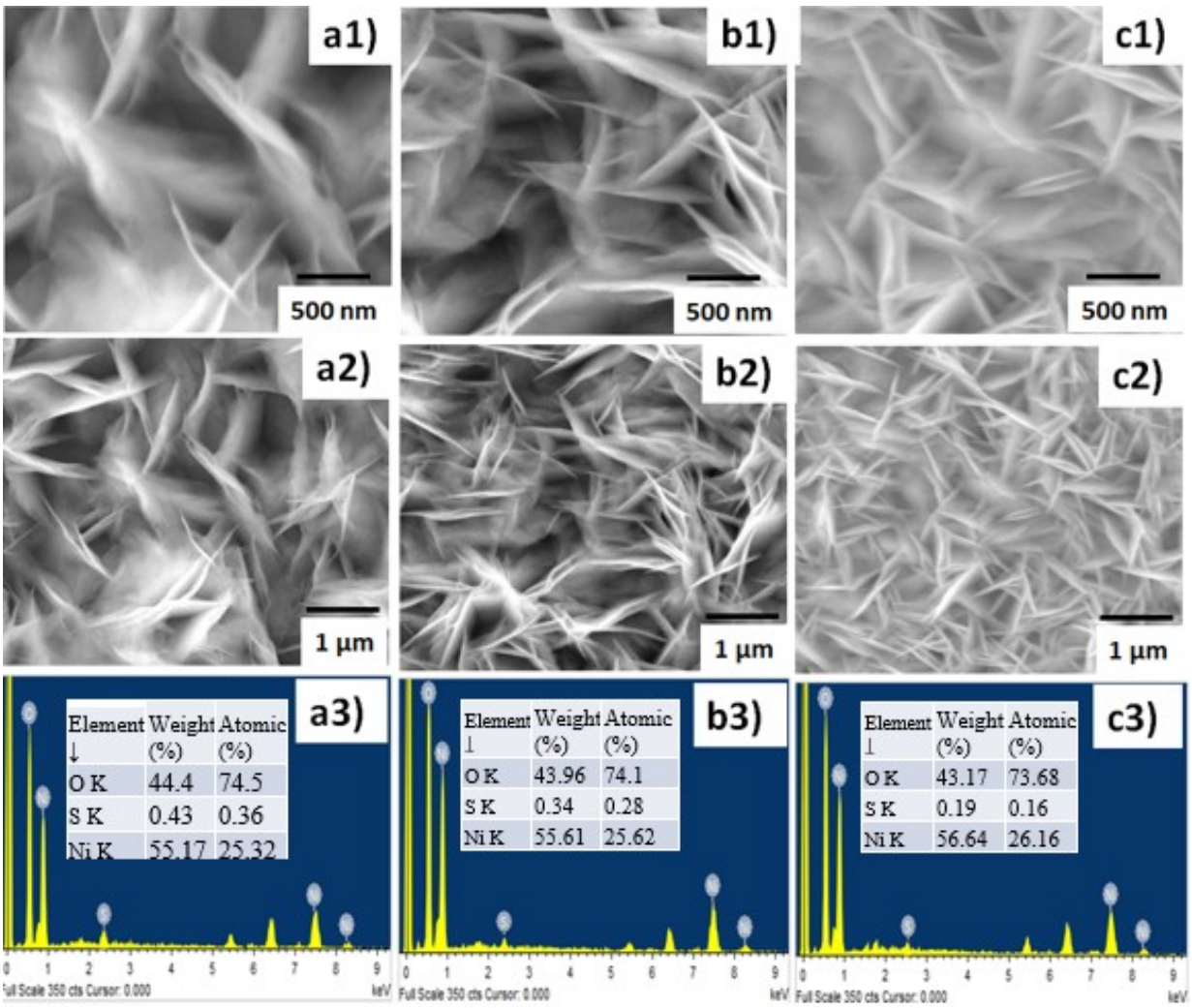

Fig. S2 FESEM Micrographs and EDS spectrum of as synthesised electrodes S1 (a1-a3), S2 (b1-b3) & S3 (c1-c3) with fuzzy morphology.

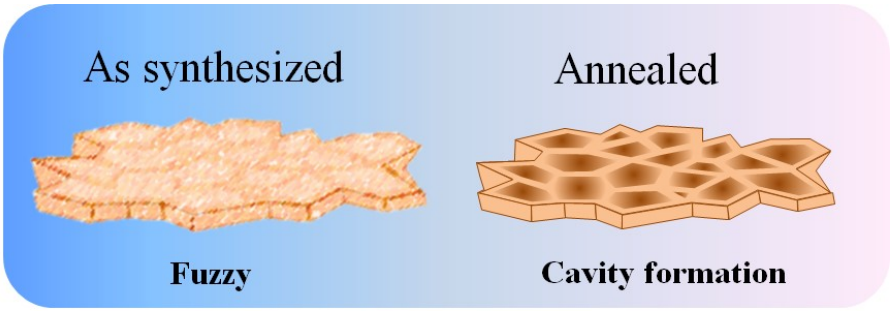

Fig. S3. Schematic representation of growth mechanism and morphological transformation.

As-synthesized electrode showed dense, fuzzy nanoflakes with a smaller thickness While annealing films significantly showed honeycomb like morphology having multiple active surfaces in the form of cavity.

Sample →	S1		**A1**		S2		**A2**		S3		**A3**	
Element ↓	Weight (%)	Atomic (%)	**Weight (%)**	**Atomic (%)**	Weight (%)	Atomic (%)	**Weight (%)**	**Atomic (%)**	Weight (%)	Atomic (%)	**Weight (%)**	**Atomic (%)**
O K	44.4	74.12	**27.53**	**57.55**	44.05	75.1	**30.52**	**61.32**	43.17	76.68	**30.82**	**61.74**
S K	0.43	0.36	**1.4**	**1.42**	0.34	0.28	**1.04**	**1.05**	0.19	0.16	**0.96**	**1.01**
Ni K	55.17	25.52	**71.07**	**41.03**	55.61	24.62	**68.44**	**37.63**	56.64	23.16	**68.22**	**37.25**

Table ST2. Comparison values of as synthesised and annealed electrodes from EDS spectrum evaluation.

3. Electrochemical properties:

3.1 Electrochemical properties influenced by annealing process of electrodes

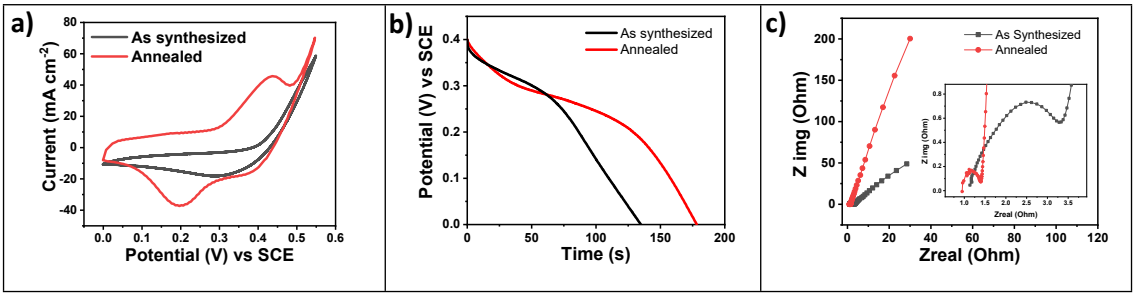

Fig S4 Comparative electrochemical performance of as synthesized S1 & annealed A1 electrode by a) CV curve at 100 mV s^{-1} b) GCD at 1 mA g^{-1} c) EIS studies

This comparison in between as deposited and annealing; evidently shows the role of annealing towards effectively enhance the electrochemical properties.

3.2 CV curves of individual electrodes:

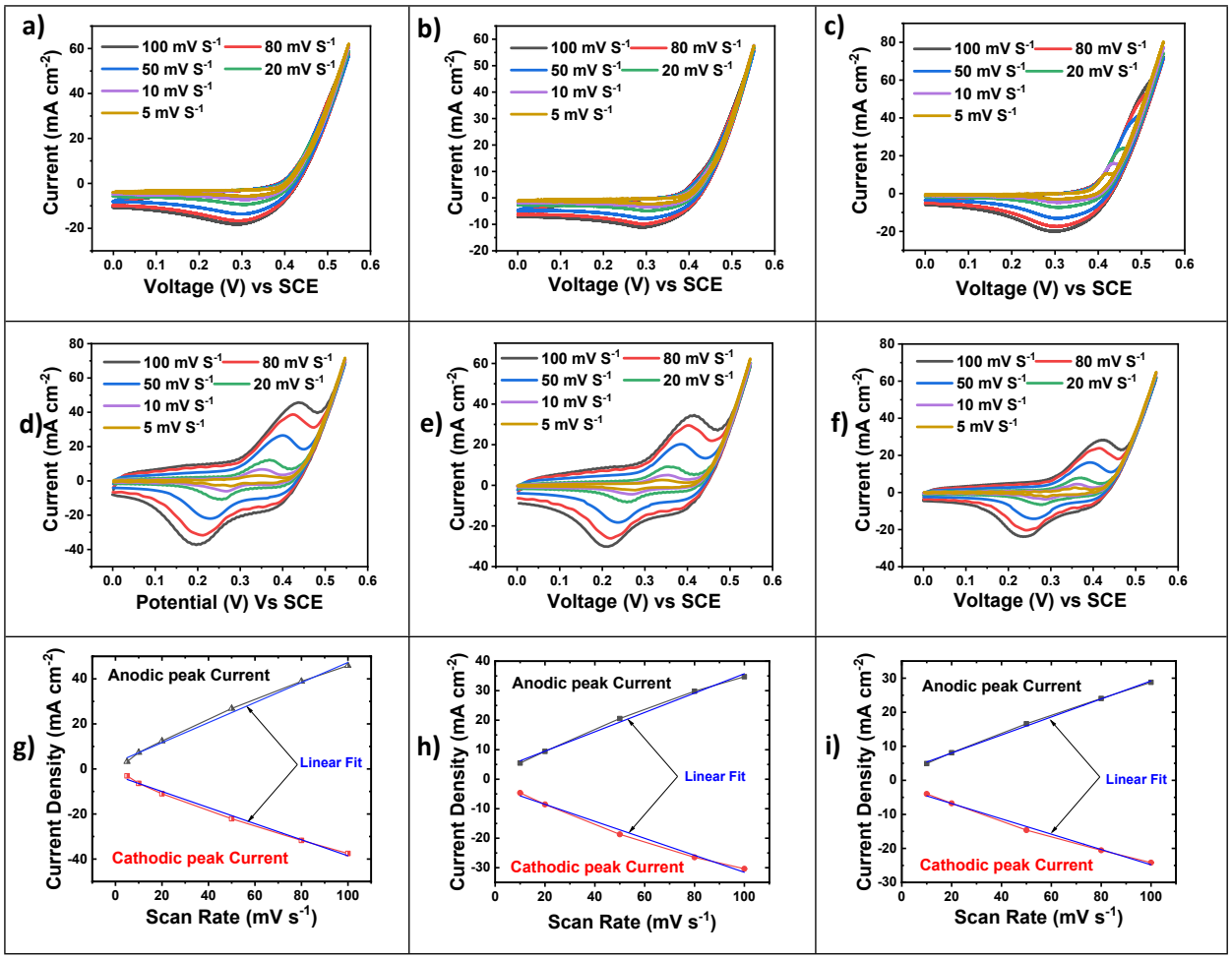

Fig S5 CV curves obtained at potential range of 0-0.55 V and scan rate of variation from 5 to 100mV/s for as synthesized a-c) S1, S2 & S3 and annealed sample d-f) A1, A2 & A3 respectively. The curves of cathodic and anodic peak current vs. scan rate g-i) for electrode A1, A2 & A3.

3.3 GD curves of individual electrode

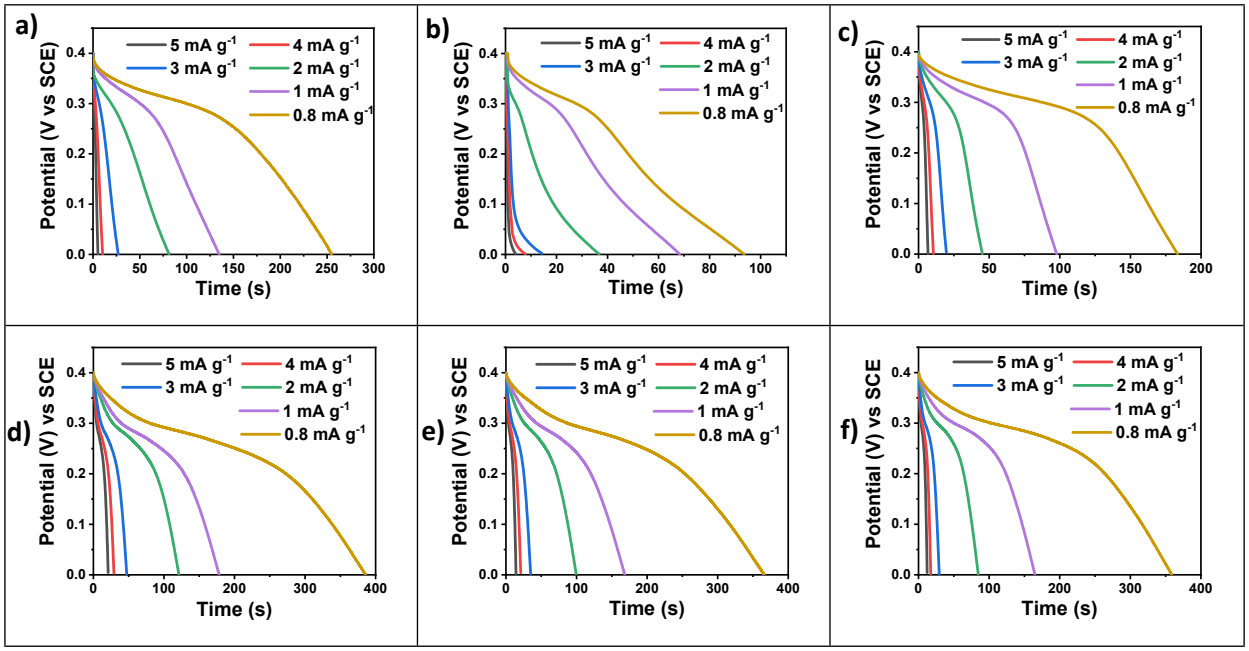

Fig S6 GD tested for as synthesized a-c) S1, S2 & S3 and annealed sample d-f) A1, A2 & A3

3.4 EIS plots of individual electrode

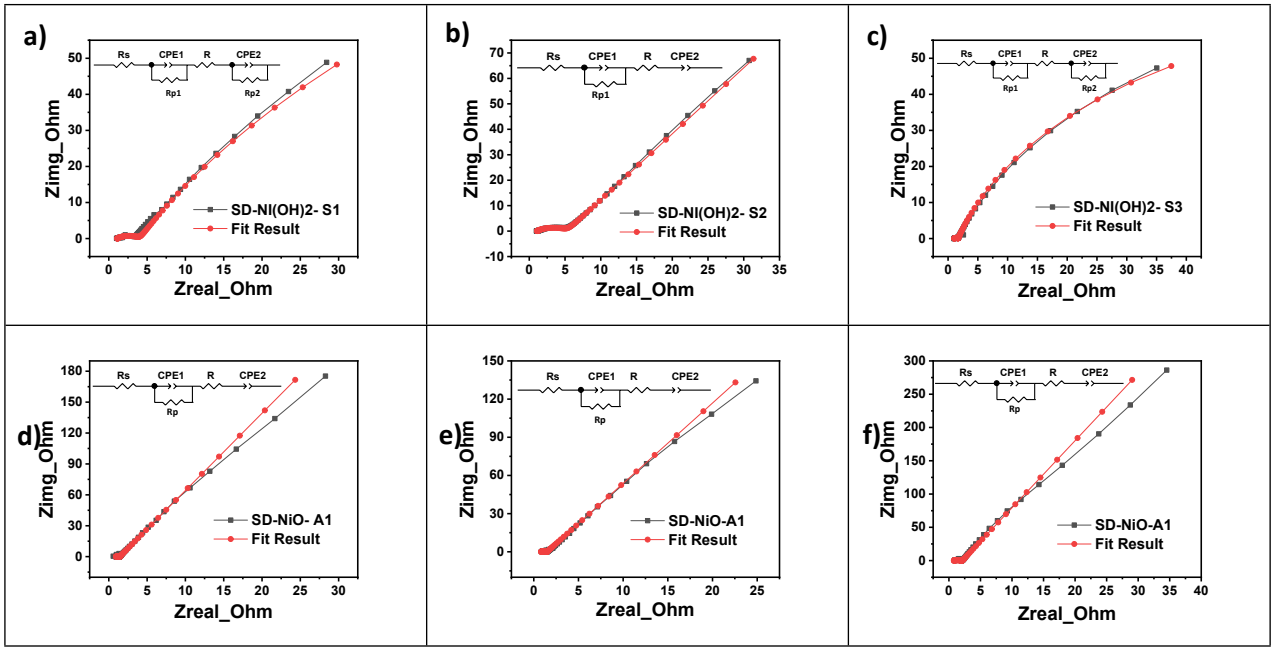

Fig S7 EIS tested and fit result with the circuits for as synthesized a-c) S1, S2 & S3 and annealed sample d-f) A1, A2 & A3

Element → **Sample ↓**	**Rs**	**CPE1-T**	**CPE1-P**	**Rp**	**CPE2-T**	**CPE2-P**
A1	0.93269	0.0019433	0.73897	**0.45674**	0.599	0.91555
A2	0.91291	0.00062727	0.71288	0.97239	0.71134	0.9
A3	0.90047	0.00024232	0.85034	1.10889	0.4132	0.93554

Table ST3 shows detail valuation of EIS plot of A1, A2 & A3 electrodes.

4. AAHSc (S-NiO// KOH// Graphite) Device performance:

a)

Current density (mA cm^{-2}) Constant	P.W. (V)	Energy density (Wh kg^{-1})	Power density (kW kg^{-1})
5	0.6	0.720193953	0.855675984
5	0.8	1.860302973	1.140901312
5	1	3.838657539	1.42612664
5	1.2	7.753375166	1.711351968
5	1.4	13.43252836	1.996577296
5	1.6	19.55378082	2.281802624
5	**1.8**	**34.96149458**	**2.567027952**

b)

Current density (mA cm^{-2}) varied	P.W. (V)	Energy density (Wh kg^{-1})	Power density (kW kg^{-1})
5	1.8	**34.96149458**	2.567027952
6	1.8	24.9087279	3.080433542
8	1.8	23.89047347	4.107244723
10	1.8	22.63262978	5.134055904
12	1.8	21.04962921	6.160867085
14	1.8	19.36679977	**7.187678266**

Table ST4. Energy and Power density values of AAHSc device a) variation of potential window (P.W.), b) variation of current density.

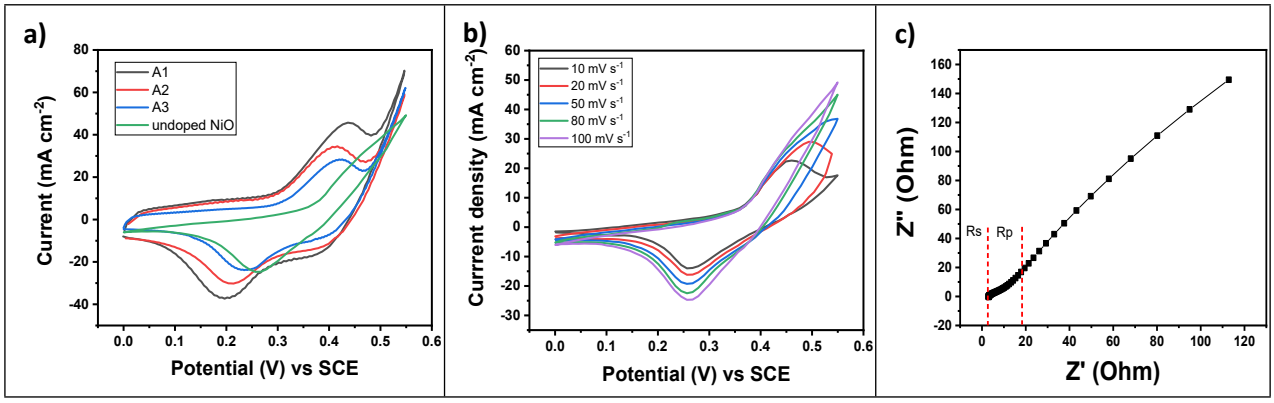

Fig. S8 (a) Comparative CV curves of undoped NiO with S-NiO (A1, A2 and A3) electrodes at scan rate of 100 mV s^{-1}. (b) CV curves at different scan rates and (c) Nyquist plot of undoped NiO electrode in 1M KOH.

From Fig. (S8 a), it is evident that, the sulfur doping electrode (A1) has significantly larger area under the CV curve with well-defined redox peaks as compared to undoped NiO electrode. This comparison significantly focuses on the effect of optimum capping delivers Ni rich active content and optimum sulfur incorporation in to NiO structure gives high performance supercapacitor electrode. The introduction of small extent of sulfur improves the exposure of active sites of electrode for the faradaic reactions owing to the enhanced surface area by honeycomb like structure. The cyclic voltammetry responses of undoped NiO at different scan rates (10–100 mV s^{-1}) over the potential window of 0.0 V – 0.55 V as shown in fig (S8 b) respectively. Specific capacitance of electrodes was calculated from CV at 20 mV s^{-1} for undoped NiO electrodes is ~278 F g^{-1}. Fig (S8 c) showed Nyquist plots in a frequency range from 0.01Hz to 10 k Hz at open circuit potential (OCP). The solution resistance (Rs) values of undoped NiO electrode are found to be 3.1 Ω, and polarization resistance (Rp) is about 13.19 Ω respectively. It is observed that, Rs and Rp values are larger than the A1 electrode, because the rapid transfer of electrons restricted by the resistive pathways and increase Rp. It generates difficulties for diffusion of electrolyte ions. Also, appropriate sulfur doping and oxygen vacancies of A1 electrode enhance electrical conductivity and contribute to high charge transfer as compared to undoped NiO electrode. Hence, role of sulfur doping is crucial in NiO electrode for superior electrochemical performance.